Received July 2004
Revised May 2005
Accepted July 2005

Effect of aspect ratio on the similarity between developing laminar flows in orthogonally rotating ducts and stationary curved ducts

Gong Hee Lee
Department of Mechanical Engineering, Pohang, Korea
Korea Institute of Nuclear Safety, Daejon, Korea, and
Je Hyun Baek
Department of Mechanical Engineering, Pohang, Korea

Abstract

Purpose – To investigate the effect of aspect ratio on the quantitative analogy between developing laminar flows in orthogonally rotating straight ducts and stationary curved ducts

Design/methodology/approach – A fractional step method is used to obtain the numerical solution of the governing equations by decoupling the solution of the momentum equations from the solution of the continuity equation. In order to clarify the similarity of the two flows, dimensionless parameters K_{LR} and Rossby number, Ro, in a rotating straight duct were used as a set corresponding to Dean number, K_{LC}, and curvature ratio, λ, in a stationary curved duct.

Findings – Under the condition that the aspect ratio was larger than one and that the magnitude of Ro or λ was large enough to satisfy the "asymptotic invariance property" the quantitative analogy between the two flows was established clearly.

Research limitations/implications – As the aspect ratio decreased below one, the difference between the secondary flow intensities of these two flows increased, and therefore, the analogy between the two flows was not as evident as that for the larger aspect ratios.

Practical implications – Based on this methodology, the characteristics of the developing flow in orthogonally rotating ducts of higher aspect ratio can be predicted by considering the flow in stationary curved ducts, and vice versa.

Originality/value – The results obtained in this study will suggest an optimal criterion for the application of this approach to the flow similarity analysis in rectangular ducts with arbitrary aspect ratios.

Keywords Centrifugal force, Laminar flow, Ductility

Paper type Research paper

Nomenclature

A	= aspect ratio =b/a	d	= pipe diameter
a	= duct width	d_h	= hydraulic diameter = $2ab/(a+b)$
b	= duct height	f	= fanning friction factor= $2\bar{\tau}_w/\rho w_m^2$

This work was partially supported by the Brain Korea 21 Project and the authors gratefully thank Dr Ishigaki for some valuable comments during the "Winter Institute Program" supported by the Japan-Korea Industrial Technology Cooperation Foundation.

International Journal of Numerical Methods for Heat & Fluid Flow
Vol. 16 No. 4, 2006
pp. 494-508

0961-5539
DOI 10.1108/09615530610653109

f_0 = friction factor for a stationary straight duct flow = 56.91/*Re*
K_{LR} = dimensionless parameter for laminar flow in a rotating duct= $Re/\sqrt{Ro}$
K_{LC} = dimensionless parameter for laminar flow in a curved duct or Dean number= $Re/\sqrt{\lambda}$
l = length scale for axial direction= $d_h/\sqrt{Ro}$ or $d_h/\sqrt{\lambda}$
p = static pressure
p^* = modified pressure= $p - \frac{1}{2}\rho\Omega^2(x^2 + z^2)$
R = mean radius of curvature
Re = Reynolds number= $w_m d_h/\nu$
Ro = Rossby number= $w_m/\Omega d_h$
u,v,w = velocity components in the direction of x, y, z
U_{SC} = velocity scale of the secondary flow (a stationary curved duct)= $w_m/\sqrt{\lambda}$
U_{SR} = velocity scale of the secondary flow (a rotating straight duct)= $w_m/\sqrt{Ro}$
V_s = secondary flow magnitude= $\sqrt{u^2 + v^2}$
w_m = mean velocity
Z_C = dimensionless axial distance of a stationary curved duct= $R\theta/(d_h\sqrt{\lambda}) = z/(d_h\sqrt{\lambda})$
Z_R = dimensionless axial distance of a rotating straight duct= $z/(d_h\sqrt{Ro})$

Greek symbols

Ω = angular velocity
ψ = stream function
λ = curvature ratio= R/d_h
ν = kinematic viscosity of the fluid
ρ = density of the fluid
θ = bending angle of a stationary curved duct

Subscript

max = maximum value

Introduction

Fluid flows in rotating and curved ducts have attracted much attention for a long time because of their relevance to various engineering applications such as cooling passages of turbine blades, blade passages of centrifugal turbomachinery, heat exchangers, and refrigeration equipments. Because of rotation and curvature effects, these examples all feature secondary flow, which not only induces the pressure drop but also results in the increased heat transfer rates.

For the flows through a straight duct subjected to a spanwise rotation, where the rotation axis is normal to the longitudinal direction of the duct, the Coriolis force throws fast-moving core flow in the direction of the cross product of the mean velocity and the rotation vectors. The near-wall flow is driven from the pressure side to the suction side of the duct along the wall regions to satisfy the continuity constraint. This onset of a secondary flow increases the friction coefficient and wall heat transfer rate. The earliest works on this subject focused on the theoretical investigation of laminar flow in a "weakly rotating" (i.e. the effect of rotation can be negligible) circular pipe. By using a perturbation expansion, Baura (1954) and Benton (1956) showed that the secondary flow consists of a counter-rotating double-vortex configuration. With a substantial increase in the rotational speed at sufficiently high Reynolds numbers, Speziale (1982) and Kheshgi and Scriven (1985) found that the usual counter-rotating double-vortex configuration breaks down into an asymmetric four-vortex configuration. Speziale and Thangam (1983) calculated the secondary flows and roll-cell instabilities in the laminar pressure-driven duct flow subjected to a spanwise rotation. They showed that there is a considerable distortion of the axial velocity profiles in the Taylor-Proudman region, resulting in a substantial reduction in the flow rate. Yang *et al.* (1994) presented a detailed review of the literature on rotating duct flow.

Analogous flow patterns can be observed in a stationary curved duct because longitudinal curvature produces a similar effect to that of spanwise rotation. When a

viscous fluid flows through a curved duct, the streamline curvature generates a centrifugal force that acts perpendicular to the primary flow direction and a secondary flow is produced. This double counter-rotating secondary flow causes the symmetric and quasi-parabolic axial velocity profile to become asymmetric, shifting the location of the maximum axial velocity outward. The first major theoretical study of laminar flow in a curved duct was performed by Dean (1927), who showed that the fully developed laminar flow in "loosely curved" (i.e. the effect of curvature can be neglected) ducts depends largely on a single dimensionless parameter, now known as the Dean number. Winters (1987) performed a linear analysis of the Dean problem, and showed that the two-vortex solution on the primary branch is stable to any arbitrary two-dimensional perturbation, while the four-vortex solution is conditionally stable to symmetric perturbations but unstable to asymmetric perturbations. Soh (1988) numerically showed that the fluid flow in a curved duct develops into different patterns, depending on the inlet condition. Thangam and Hur (1990) found that for ducts of small curvature ratio the onset of transition from single vortex pair to double vortex or roll cells depends on the Dean number and the curvature ratio, while for ducts of large curvature ratio the onset can be characterized only by the Dean number. They also proposed a correlation for the friction factor as a function of the Dean number and aspect ratio. Berger *et al.* (1983) and Ito (1987) extensively reviewed the results of previous studies concerning the secondary flow in a curved pipe.

To the best of the author's knowledge, most previous studies of the analogy between the flows through orthogonally rotating straight ducts and stationary curved ducts have been qualitatively performed only for a circular cross section (Trefethen, 1957; Ito, 1959; Ito and Nanbu, 1971). In the case of rectangular ducts, the aspect ratio (i.e. the ratio of the duct height to its width) is one of the dominant geometric constraints which affect the secondary flow patterns. Moore (1967) revealed that the influence of rotation on velocity profiles and wall shear stresses is quite large at low aspect ratios, whereas a much smaller effect is observed at high aspect ratios. Jen and Lavine (1992) numerically investigated the effect of aspect ratio on the laminar heat transfer and fluid flow in the entrance region of a rotating duct. They showed that the number of vortex pairs strongly depend on the aspect ratio of the duct.

The objective of the present study is to investigate the effect of aspect ratio on the quantitative analogy between developing laminar flows in orthogonally rotating straight ducts and stationary curved ducts using a fractional step solver and the dimensionless parameters, successfully validated in previous papers (Lee and Baek, 2002a, b). It is expected that the results obtained in this study will suggest an optimal criterion for the application of this approach to the flow similarity analysis in rectangular ducts with arbitrary aspect ratios.

Governing equations

Figure 1(a) and (b) show the geometry of the physical model and its coordinate system used for flow analysis in a rotating straight duct and a stationary curved duct of rectangular cross-section, respectively. In a previous paper (Lee and Baek, 2001), governing parameters were driven by applying appropriately scaled variables (Ishigaki, 1999) to the Navier-Stokes equations. For simplicity, only the dimensionless forms of the governing equations for the developing laminar flows of an

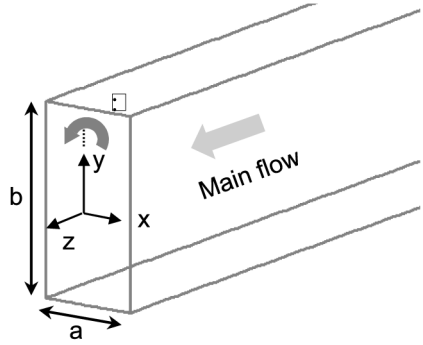

(a) Rotating straight duct

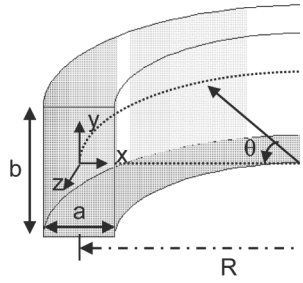

(b) Stationary curved duct

Figure 1.
Geometric configuration and coordinate system for flow analysis

incompressible Newtonian fluid are considered herein (see Ishigaki (1999) for circular pipe flows).

Rotating straight duct

As shown in Figure 1(a), the Cartesian coordinate system fixed to a straight duct that rotates about the y-axis at a constant angular velocity Ω is used. The relative velocity components in the direction of increasing (x,y,z) are denoted by (u,v,w). Here, u and v are the velocity components of secondary flow in a cross-section, while w represents the primary flow.

The following dimensionless variables are used to derive the dimensionless governing equations (3)-(6):

$$\tilde{t} = \frac{w_{\mathrm{m}}}{d_{\mathrm{h}}\sqrt{Ro}}t, \quad \tilde{u} = \frac{u}{w_{\mathrm{m}}}\sqrt{Ro}, \quad \tilde{v} = \frac{v}{w_{\mathrm{m}}}\sqrt{Ro}, \quad \tilde{w} = \frac{w}{w_{\mathrm{m}}}, \quad \tilde{p}^{*} = \frac{p^{*}}{\rho w_{\mathrm{m}}^{2}}Ro,$$
$$\tilde{x} = \frac{x}{d_{\mathrm{h}}}, \quad \tilde{y} = \frac{y}{d_{\mathrm{h}}}, \quad \tilde{z} = \frac{z}{l} = \frac{z}{d_{\mathrm{h}}\sqrt{Ro}} \tag{1}$$

where w_{m} is the mean velocity, d_{h} is the hydraulic diameter of the rectangular duct defined as $d_{\mathrm{h}} = 2ab/(a+b)$, where a is the duct width and b is the duct height. The modified pressure p^{*} is given by:

$$p^* = p - \frac{1}{2}\rho\Omega^2(x^2 + z^2) \tag{2}$$

and the Rossby number, $Ro = w_m/\Omega d_h$, is a convenient parameter for quantifying the relative strength of the inertial force to the Coriolis force acting on the fluid. Another dimensionless parameter $K_{LR} = Re/\sqrt{Ro}$ represents the Reynolds number based on the velocity scale of the secondary flow $U_{SR} = w_m/\sqrt{Ro}$ and length scale d_h. If "weakly rotating" duct flow is assumed for $Ro \geq 10$ (Ito and Nanbu, 1971), the limiting forms of the governing equations do not include Ro, and the flow characteristics of the rotating duct are governed only by K_{LR}. This means that the flow fields exhibit an "asymptotic invariance property" of Ro:

$$\frac{\partial \tilde{u}}{\partial \tilde{x}} + \frac{\partial \tilde{v}}{\partial \tilde{y}} + \frac{\partial \tilde{w}}{\partial \tilde{z}} = 0 \tag{3}$$

$$\frac{\partial \tilde{u}}{\partial \tilde{t}} + \tilde{u}\frac{\partial \tilde{u}}{\partial \tilde{x}} + \tilde{v}\frac{\partial \tilde{u}}{\partial \tilde{y}} + \tilde{w}\frac{\partial \tilde{u}}{\partial \tilde{z}} = -\frac{\partial \tilde{p}^*}{\partial \tilde{x}} + \frac{1}{K_{LR}}\left(\frac{\partial^2 \tilde{u}}{\partial \tilde{x}^2} + \frac{\partial^2 \tilde{u}}{\partial \tilde{y}^2}\right) + 2\tilde{w} \tag{4}$$

$$\frac{\partial \tilde{v}}{\partial \tilde{t}} + \tilde{u}\frac{\partial \tilde{v}}{\partial \tilde{x}} + \tilde{v}\frac{\partial \tilde{v}}{\partial \tilde{y}} + \tilde{w}\frac{\partial \tilde{v}}{\partial \tilde{z}} = -\frac{\partial \tilde{p}^*}{\partial \tilde{y}} + \frac{1}{K_{LR}}\left(\frac{\partial^2 \tilde{v}}{\partial \tilde{x}^2} + \frac{\partial^2 \tilde{v}}{\partial \tilde{y}^2}\right) \tag{5}$$

$$\frac{\partial \tilde{w}}{\partial \tilde{t}} + \tilde{u}\frac{\partial \tilde{w}}{\partial \tilde{x}} + \tilde{v}\frac{\partial \tilde{w}}{\partial \tilde{y}} + \tilde{w}\frac{\partial \tilde{w}}{\partial \tilde{z}} = -\frac{\partial \tilde{p}^*}{\partial \tilde{z}} + \frac{1}{K_{LR}}\left(\frac{\partial^2 \tilde{w}}{\partial \tilde{x}^2} + \frac{\partial^2 \tilde{w}}{\partial \tilde{y}^2}\right) \tag{6}$$

Stationary curved duct

Figure 1(b) shows a toroidal coordinate system $(x, y, z = R\theta)$ where the radius of curvature along the duct centerline is represented by R and the finite pitch effect is negligible. The corresponding absolute velocity components in the radial, spanwise, and axial direction are represented by (u,v,w), respectively. By applying a similar procedure that used previously in the analysis of a rotating straight duct, the following non-dimensional variables are used to derive the dimensionless governing equations (8)-(11).

$$\tilde{t} = \frac{w_m}{d_h\sqrt{\lambda}}t, \quad \tilde{u} = \frac{u}{w_m}\sqrt{\lambda}, \quad \tilde{v} = \frac{v}{w_m}\sqrt{\lambda}, \quad \tilde{w} = \frac{w}{w_m}, \quad \tilde{p} = \frac{p}{\rho w_m^2}\lambda, \quad \tilde{x} = \frac{x}{d_h},$$
$$\tilde{y} = \frac{y}{d_h}, \quad \tilde{z} = \frac{z}{l} = \frac{z}{d_h\sqrt{\lambda}} \tag{7}$$

where $\lambda = R/d_h$ is the curvature ratio that is an indication of the ratio between the inertial force and the centrifugal force. In equations (9)-(11), $K_{LC} = Re/\sqrt{\lambda}$ represents the Dean number that provides a measure of the intensity of the secondary flow. Previous research on finite curvature effects (Ito, 1959; Austin and Seader, 1973)

demonstrated that the effects of the curvature ratio are practically negligible (i.e. loosely curved) when λ is larger than about eight. Therefore, under those conditions, equations (8)-(11) are not a function of λ and the flow features exhibit an "asymptotic invariance property" of λ. This means that K_{LC} is the sole governing parameter. As a result, the governing equations (3)-(6) for a "weakly rotating" duct flow are similar to those of equations (8)-(11) for a "loosely curved" duct flow, except for body force terms in equations (4) and (9):

$$\frac{\partial \tilde{u}}{\partial \tilde{x}} + \frac{\partial \tilde{v}}{\partial \tilde{y}} + \frac{\partial \tilde{w}}{\partial \tilde{z}} = 0 \tag{8}$$

$$\frac{\partial \tilde{u}}{\partial \tilde{t}} + \tilde{u}\frac{\partial \tilde{u}}{\partial \tilde{x}} + \tilde{v}\frac{\partial \tilde{u}}{\partial \tilde{y}} + \tilde{w}\frac{\partial \tilde{u}}{\partial \tilde{z}} = -\frac{\partial \tilde{p}}{\partial \tilde{x}} + \frac{1}{K_{LC}}\left(\frac{\partial^2 \tilde{u}}{\partial \tilde{x}^2} + \frac{\partial^2 \tilde{u}}{\partial \tilde{y}^2}\right) + \tilde{w}^2 \tag{9}$$

$$\frac{\partial \tilde{v}}{\partial \tilde{t}} + \tilde{u}\frac{\partial \tilde{v}}{\partial \tilde{x}} + \tilde{v}\frac{\partial \tilde{v}}{\partial \tilde{y}} + \tilde{w}\frac{\partial \tilde{v}}{\partial \tilde{z}} = -\frac{\partial \tilde{p}}{\partial \tilde{y}} + \frac{1}{K_{LC}}\left(\frac{\partial^2 \tilde{v}}{\partial \tilde{x}^2} + \frac{\partial^2 \tilde{v}}{\partial \tilde{y}^2}\right) \tag{10}$$

$$\frac{\partial \tilde{w}}{\partial \tilde{t}} + \tilde{u}\frac{\partial \tilde{w}}{\partial \tilde{x}} + \tilde{v}\frac{\partial \tilde{w}}{\partial \tilde{y}} + \tilde{w}\frac{\partial \tilde{w}}{\partial \tilde{z}} = -\frac{\partial \tilde{p}}{\partial \tilde{z}} + \frac{1}{K_{LC}}\left(\frac{\partial^2 \tilde{w}}{\partial \tilde{x}^2} + \frac{\partial^2 \tilde{w}}{\partial \tilde{y}^2}\right) \tag{11}$$

Numerical method

A fractional step method is used to obtain the numerical solution of the governing equations by decoupling the solution of the momentum equations from the solution of the continuity equation. In the present method, the calculation is carried out in two steps. The first step (convection-diffusion step) solves for an intermediate velocity field (with the pressure gradients omitted) by advancing the momentum equations in time with an implicit ADI method. Then, in order to obtain a divergence-free velocity field, the velocities are corrected by the pressure gradients at the next time step until the continuity equation is satisfied (continuity step). For a steady flow analysis, the solution is advanced in pseudo-time until a converged solution is obtained. The viscous and pressure gradient terms are discretized using second-order accurate central differencing, while second-order accurate upwind differencing is used to minimize the cross-stream numerical diffusion for the convective term. To accelerate the convergence of the solution to the steady state, locally varying time steps are applied to the Navier-Stokes equations. The use of a collocated grid simplifies the implementation of boundary conditions and reduces the additional storage requirements of the solution variables. At the duct inlet, uniform flow is imposed. No slip boundary condition is applied at the wall. At the duct exit, second order extrapolation for velocities is employed.

The solution is assumed to be converged when the residuals of the solution variables between the current and previous time steps display the six orders of the

magnitude drop. A more detailed description of the numerical scheme can be found in Constantinescu and Patel (1998).

Since, there may be an asymmetric pattern of longitudinal vortices in the cross sections of the duct as the flow proceeds downstream (Jen and Lavine, 1992), the present computations are performed over the entire cross-section. Four different grid sizes for an aspect ratio $A = b/a = 2$ were used to check the grid independence of the numerical solution. The grid sizes are $100 \times 25 \times 49$, $100 \times 35 \times 69$, $100 \times 45 \times 89$ and $150 \times 35 \times 69$ in the axial, horizontal and vertical direction, respectively. A non-uniform grid with clustering at the entrance and in the near wall region was used because the velocity for both the main and secondary flow changes rapidly in these regions.

Figure 2 shows the axial variation of the dimensionless maximum axial velocity and the averaged friction factor ratio. Increasing the grid size in the axial direction shows a negligible difference in the predicted results. Considering the computational time and the solution accuracy, a grid size of $100 \times 35 \times 69$ was selected for $A = 2$. A similar grid dependence study was also conducted for the different aspect ratios and the final grid sizes are summarized in Table I.

Results and discussion

To investigate the effect of aspect ratio on the analogy between developing laminar flows in an orthogonally rotating straight duct and a stationary curved duct of rectangular cross-section under the condition that the magnitudes of Ro and λ are large enough for the flow field to satisfy the "asymptotic invariance property" four different aspect ratios $A = 0.25$, 0.5, 2 and 4 are considered at $K_{LR} = K_{LC} = 125$ and $Ro = \lambda = 20$. Since, the results on the flow similarity for $A = 1$ were fully presented in a separate paper (Lee and Baek, 2001), they are not considered here.

General flow patterns

Figure 3 shows the dimensionless axial velocity (w/w_m) contours. The upper half of each duct cross-section shows the stationary curved duct flow, while the lower half shows the rotating straight duct flow. Therefore, the pressure and suction sides in a rotating duct flow correspond to the outer (convex) and inner (concave) wall of a stationary curved duct flow, respectively. For the rotating straight duct flow, as the dimensionless axial distance Z_R increases, by the action of the Coriolis force, the high-momentum fluid originally located in the central core is convected to the pressure side of the duct, significantly reducing the thickness of the boundary layers along the top, bottom and pressure sides, while the low-momentum fluid accumulates along the suction side, causing the boundary layer thickness to increase there.

In the stationary curved duct flow, similar to the rotating straight duct flow, as the dimensionless axial distance Z_C increases, the location of the maximum axial velocity shifts toward the outer wall due to the effect of the centrifugal force that acts outwards from the center of curvature. For $A < 1$ ($A = 0.25$ and 0.5), the difference between the axial velocity distributions for the rotating straight duct and the stationary curved duct increases as the fluid proceeds downstream. On the other hand, the axial velocity contours for the two flows are overall coincident for $A > 1$ ($A = 2$ and 4).

Figure 4 shows the secondary velocity vectors in the cross-section at the same axial distances as those used in Figure 3. For the rotating duct, the secondary flow consists

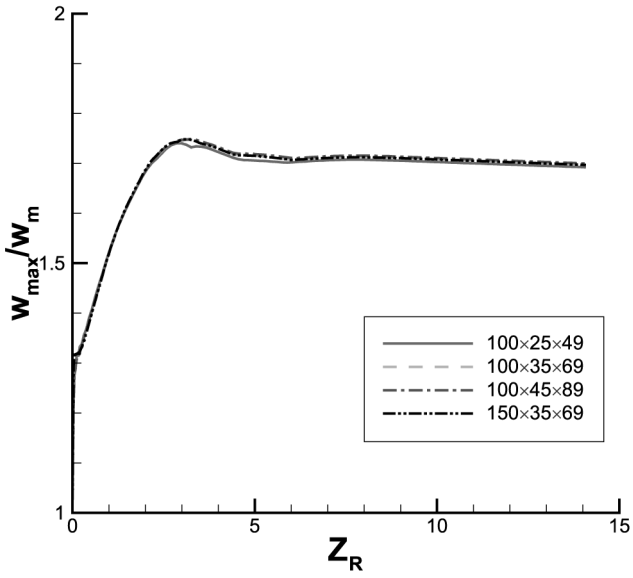

(a)

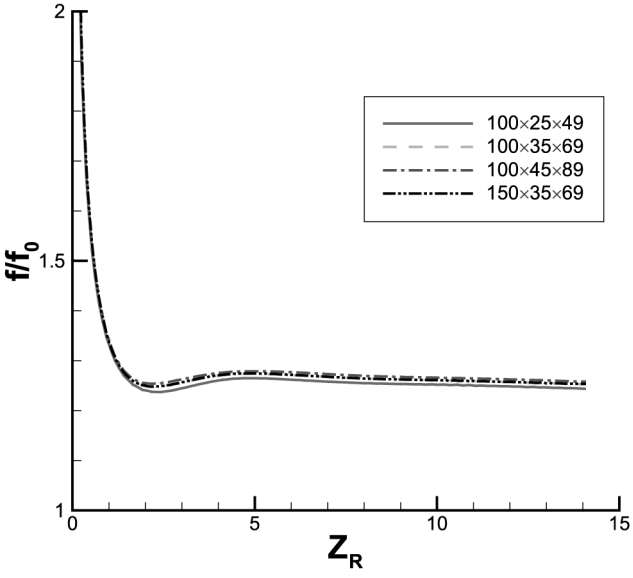

(b)

Figure 2.
Grid independency check: axial variation of (a) the maximum axial velocity and (b) the averaged friction factors for $A = 2, K_{LR} = 125$ and $Ro = 20$

of a counter-rotating double-vortex configuration due to the effect of the Coriolis force. In the stationary curved duct, since the centrifugal force is proportional to the square of the axial velocity at a given position, the high momentum flow in the central core region is subjected to a larger centrifugal force than the slower-moving fluid near the duct walls. A counter-rotating double vortex is generated to satisfy a momentum balance and continuity. The two flows have similar secondary flow patterns.

Table I. Grid system

	Aspect ratio ($A = b/a$)			
	0.25	0.5	2	4
Grid size				
Axial	100	100	100	100
Radial	139	69	35	35
Spanwise	35	35	69	139

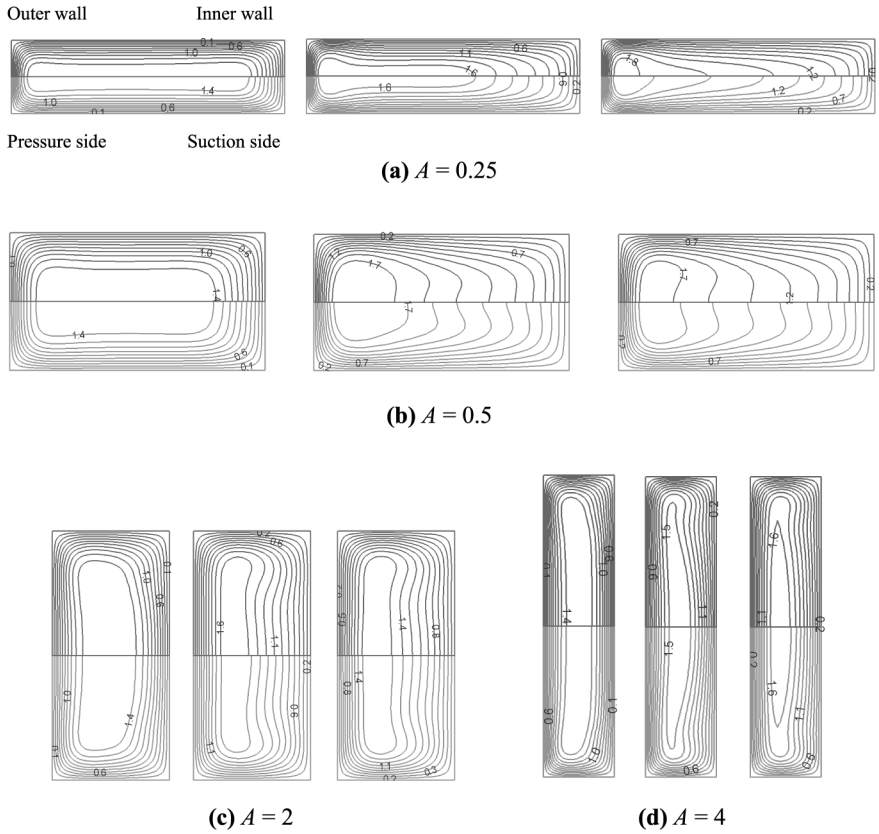

Figure 3. Development of dimensionless axial velocity contours at $K_L = 125$ and $Ro = \lambda = 20$ (upper: stationary curved duct, lower: rotating straight duct): $Z = 1.16$(left); $Z = 3.12$(center); $Z = 12.6$(right)

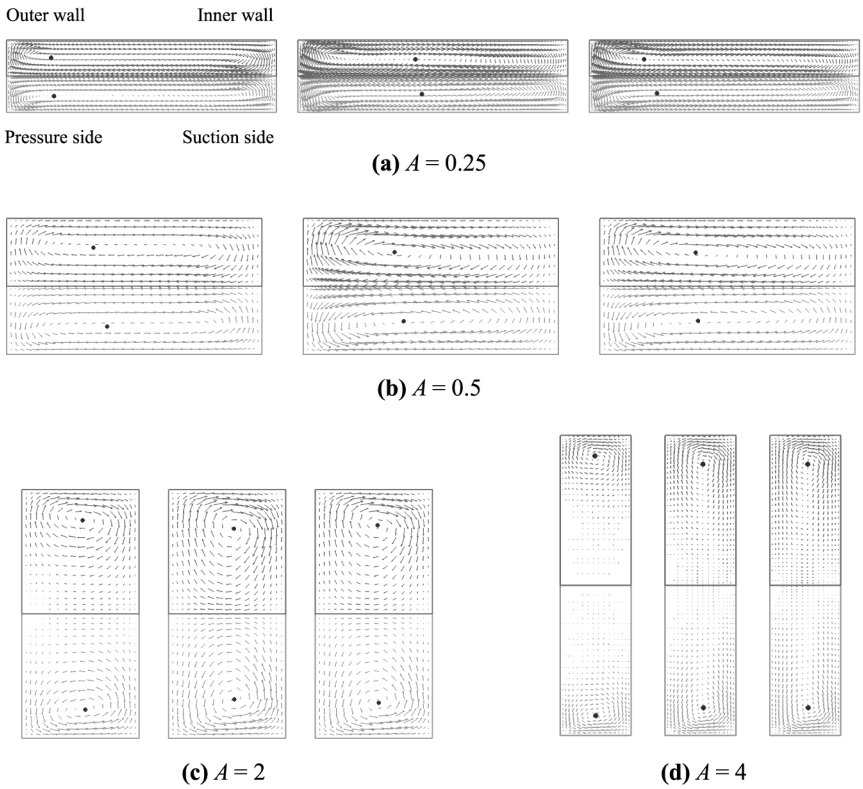

Figure 4.
Development of secondary velocity vectors at $K_L = 125$ and $Ro = \lambda = 20$ (upper: stationary curved duct, lower: rotating straight duct); $Z = 1.16$(left); $Z = 3.12$(center); $Z = 12.6$(right)

Friction factor

One of the most important practical aspects of duct flow is an accurate prediction of the friction factor for calculating the pressure loss. Figure 5 shows the axial variation of the averaged friction factors of these two flows. The friction factors are normalized by the corresponding value for fully developed flow in a stationary straight duct.

For the same cross-sectional area, the friction factor ratio at the lower aspect ratios has a much larger value in the fully developed flow region where the friction factor ratio approaches a constant value. The reason may be that the enhanced effects of rotation and curvature at lower aspect ratio increase the intensity of the secondary flow. The predicted friction factors for the two flows show overall good agreement.

Other flow features

Figure 6 shows the axial variation of the maximum axial velocity (w_{max}/w_m). For $A > 1$ the velocity magnitudes for each flow are nearly the same, but the difference between the magnitudes increases as the aspect ratio is made smaller than one.

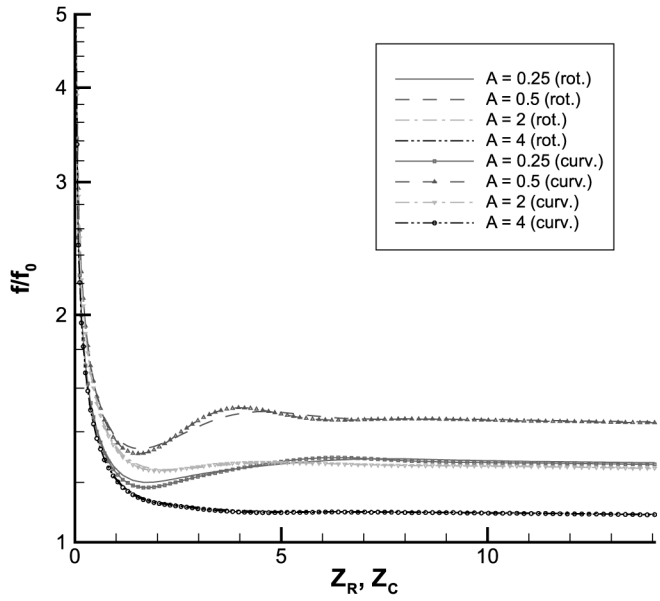

Figure 5.
Axial variation of average friction factor ratio at $K_L = 125$ and $Ro = \lambda = 20$

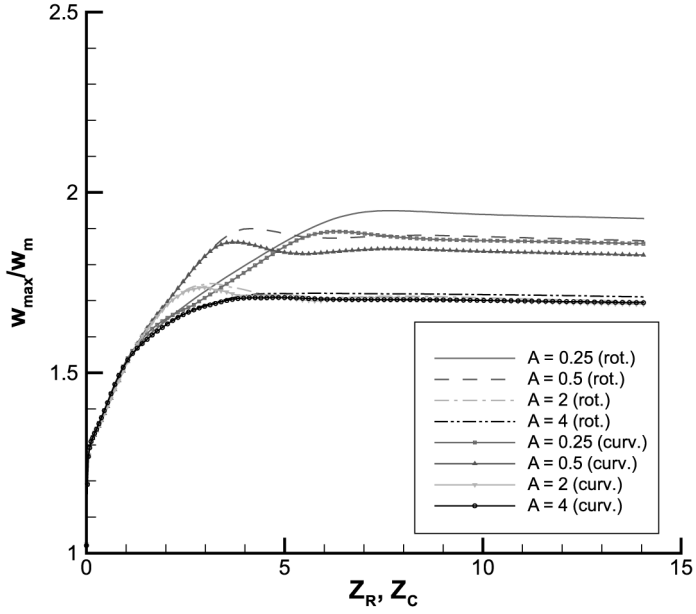

Figure 6.
Axial variation of maximum axial velocity ratio at $K_L = 125$ and $Ro = \lambda = 20$

The axial variation of the normalized maximum value of the secondary flow velocity V_{Smax} (so-called the intensity of the secondary flow) is shown in Figure 7. The difference between V_{Smax} for the two flows is greater than that of an integral property such as the friction factor (Figure 5). The reason is that, as can be seen in equation (4) and (9), the Coriolis force acting on the fluid is proportional to its velocity, whereas the centrifugal force acting on the fluid is proportional to the square of its velocity, and thus the intensities of the secondary flow have a local discrepancy in the cross-sectional plane. As the aspect ratio decreases, the magnitude of secondary flow intensity and its difference between the two flows increase. The increasing difference between the secondary flows for the two flows at the lower aspect ratios may explain the difference between the axial velocity distributions, as shown in Figure 3.

The axial variation of the normalized maximum value of the stream function ψ_{max} is shown in Figure 8. The maximum value is located at the vortex center represented by a solid circle in Figure 4. For the same cross-section area, ψ_{max} has a relatively large value at the smaller aspect ratio. In the fully developed region, ψ_{max} has the largest value at $A = 0.5$ and the smallest value at $A = 4$. The difference of ψ_{max} between the two flows increases as the aspect ratio decreases.

Conclusions

A numerical study was performed in order to investigate the effect of aspect ratio on the quantitative analogy between developing laminar flows in orthogonally rotating straight ducts and stationary curved ducts of rectangular cross-section. Based on the results obtained in this study, the following conclusions could be drawn:

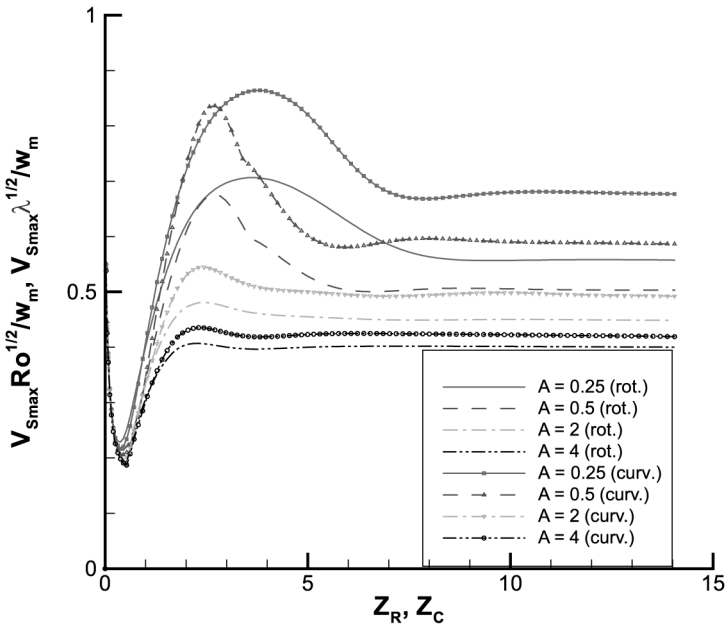

Figure 7.
Axial variation of maximum secondary velocity intensity at $K_L = 125$ and $Ro = \lambda = 20$

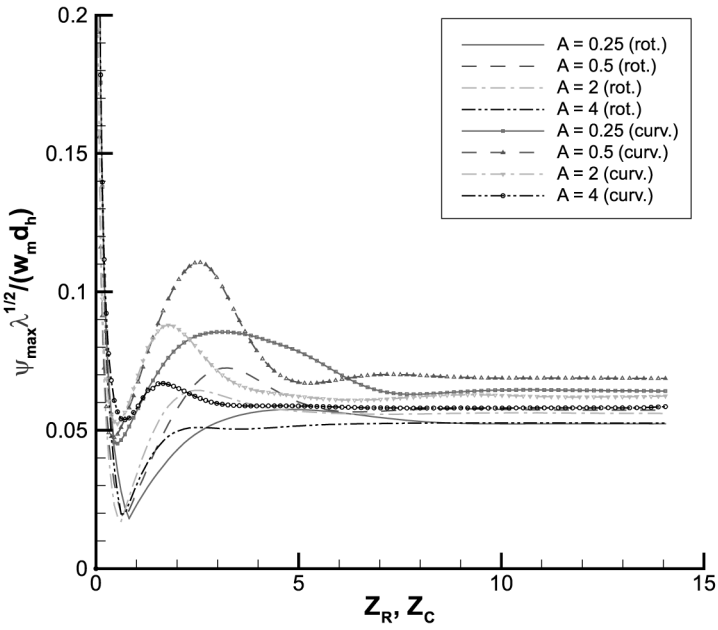

Figure 8.
Axial variation of maximum value of stream function at $K_L = 125$ and $Ro = \lambda = 20$

- The validity of the similarity parameters suggested by Trefethen (1957) and Ishigaki (1999) for circular pipe flow was confirmed for the flows through the rectangular ducts with aspect ratio $A \geq 1$. That is, K_{LR} and the Rossby number, Ro, for the laminar flow in orthogonally rotating ducts correspond to the Dean number, K_{LC}, and the curvature ratio, λ, for stationary curved rectangular duct flows. Here, the hydraulic diameter, d_h, was used instead of the pipe diameter, d.
- Under the condition that the aspect ratio was larger than one and that the magnitude of Ro or λ was large enough to satisfy the "asymptotic invariance property" the quantitative analogy between the two flows was established clearly. Primary and secondary flow patterns and friction factors were similar for the same values of K_{LR} and K_{LC}.
- As the aspect ratio decreased below one ($A = 0.25$ and 0.5), the difference between the secondary flow intensities of these two flows increased, and therefore, the analogy between the two flows was not as evident as that for the larger aspect ratios ($A = 2$ and 4).
- Based on this methodology, the characteristics of the developing flow in orthogonally rotating ducts of higher aspect ratio can be predicted by considering the flow in stationary curved ducts, and vice versa.

References

Austin, L.R. and Seader, J.D. (1973), "Fully developed viscous flow in coiled circular pipes", *AIChE Journal*, Vol. 19, pp. 85-93.

Baura, S.N. (1954), "Secondary flow in a rotating straight pipe", *Proceedings of the Royal Society of London*, Vol. A 227, pp. 133-9.

Benton, G.S. (1956), "The effect of the earth's rotation on laminar flow in pipes", *Journal of Applied Mechanics*, Vol. 23, pp. 123-7.

Berger, S.A., Tabolt, L. and Yao, L-S. (1983), "Flow in curved pipes", *Annual Review of Fluid Mechanics*, Vol. 15, pp. 461-512.

Constantinescu, G. and Patel, V.C. (1998), "A numerical model for simulation of pump-intake flow and vortices", *ASCE Journal of Hydraulic Engineering*, Vol. 124, pp. 123-34.

Dean, W.R. (1927), "Note on the motion of fluid in a curved pipe", *Philosophical Magazine*, Vol. 4, pp. 208-23.

Ishigaki, H. (1999), "Analogy between developing laminar flows in curved pipes and orthogonally rotating pipes", *JSME International Journal (B)*, Vol. 42, pp. 197-205.

Ito, H. (1959), "Friction factors for turbulent flow in curved pipes", *ASME Journal of Basic Engineering*, Vol. 81, pp. 123-34.

Ito, H. (1987), "Flow in curved pipes", *JSME International Journal (B)*, Vol. 30, pp. 543-52.

Ito, H. and Nanbu, K. (1971), "Flow in rotating straight pipes of circular cross section", *ASME Journal of Basic Engineering*, Vol. 93, pp. 383-94.

Jen, T-C. and Lavine, A.S. (1992), "Laminar heat transfer and fluid flow in the entrance region of a rotating duct with rectangular cross section: the effect of aspect ratio", *ASME Journal of Heat Transfer*, Vol. 114, pp. 574-81.

Kheshgi, H.S. and Scriven, L.E. (1985), "Viscous flow through a rotating square channel", *Physics of Fluids*, Vol. 28, pp. 2868-979.

Lee, G.H. and Baek, J.H. (2001), "A numerical study on the similarity of the developing laminar flows between in orthogonally rotating square duct and stationary curved square duct", *Journal of Computational Fluids Engineering*, Vol. 6, pp. 21-30 (in Korean).

Lee, G.H. and Baek, J.H. (2002a), "A numerical study of the similarity of fully developed laminar flows in orthogonally rotating rectangular ducts and stationary curved rectangular ducts of arbitrary aspect ratio", *Computational Mechanics*, Vol. 29, pp. 183-90.

Lee, G.H. and Baek, J.H. (2002b), "A numerical study on the similarity of fully developed turbulent flows between in orthogonally rotating square ducts and stationary curved square ducts", *International Journal of Numerical Methods for Heat & Fluid Flow*, Vol. 12, pp. 241-57.

Moore, J. (1967), "Effects of Coriolis on turbulent flow in rotating rectangular channels", Report No. 89, Gas Turbine Laboratory, Massachusetts Institute of Technology, Cambridge, MA.

Soh, W.Y. (1988), "Developing fluid flow in a curved duct of square cross-section and its fully developed dual solutions", *Journal of Fluid Mechanics*, Vol. 188, pp. 337-61.

Speziale, C.G. (1982), "Numerical study of viscous flow in rotating rectangular ducts", *Journal of Fluid Mechanics*, Vol. 122, pp. 251-71.

Speziale, C.G. and Thangam, S. (1983), "Numerical study of secondary flows and roll-cell instabilities in rotating channel flow", *Journal of Fluid Mechanics*, Vol. 130, pp. 377-95.

Thangam, S. and Hur, N. (1990), "Laminar secondary flows in curved rectangular ducts", *Journal of Fluid Mechanics*, Vol. 217, pp. 421-40.

Trefethen, L.M. (1957), "Flow in rotating radial ducts", Report No. 55GL350-A, General Electric Company, Fairfield, CT.

Winters, K.H. (1987), "A bifurcation study of laminar flow in a curved tube of rectangular cross-section", *Journal of Fluid Mechanics*, Vol. 180, pp. 343-69.

Yang, W.J., Fann, S. and Kim, J.H. (1994), "Heat and fluid flow inside rotating channels", *ASME Applied Mechanics Review*, Vol. 47, pp. 367-96.

Further reading

Hur, N. (1988), "Numerical study of secondary flows in curved ducts", PhD dissertation, Stevens Institute Technology.

Corresponding author
Gong Hee Lee can be contacted at: ghlee@kins.re.kr